

Numerical simulation of flow around S-shaped rotor with slits on the blade

Yuka Yoshida and Tetuya Kawamura

(Received November 1, 2012)

Abstract

Two-dimensional flows around an S-shaped rotor that is one variation of Savonius rotor is investigated numerically by solving the incompressible Navier-Stokes equations. The fractional step method is used to solve the equations. The numerical simulation is conducted about the simple structure S-shaped rotor with the slit near the tip of the blade to understand the characteristics of the rotor by examination of the torque and the flow around the rotor. As the result of the calculations, the improvement of the power coefficient is found by providing the slit on the blade.

1. Introduction

S-shaped rotor is a kind of drag-type wind turbine which has an S-shaped plate as shown in Fig 1. The S-shaped rotor has a structure to obtain the torque by utilizing the difference in drag acting on the convex side and a concave side. The various studies have been done for Savonius rotor⁽¹⁾ which is a kind of S-shaped rotor.^{(2), (3)}

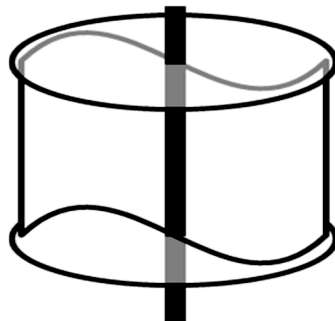


Fig. 1 S-shaped rotor

Since the power generation efficiency is low, S-shaped rotor generator is not famous in the point of the efficiency, there is an advantage to be able to form the structure by the simple process of bending the plate. On the other hand, the drag type rotor has properties of low rpm and high torque that will be suitable for using as a pumping or a powder milling. In addition, the vertical axis type rotor has good starting characteristics. S-shaped rotor can be rotated by the wind from all directions except for the specific narrow range of the wind direction at startup.

S-shaped rotor has good startup characteristics that is independent on the wind direction, and rotates in low-speed, therefore S-shaped rotor has been considered to be combined with a Darrieus type rotor which is a lift type vertical axis rotor for power generation or a straight-bladed vertical axis rotor. S-shaped rotor can be improved the startup characteristics of the lift type rotor and also expected to work as a brake when the rotation speed is too high.

The large number of the research has been done on the Savonius rotor.⁽²⁾⁻⁽⁵⁾ Ishimatsu et al⁽³⁾ carried out the comparison of the Savonius type and the S-shaped by using a numerical simulation. Yokomizo et al⁽⁵⁾ investigates experimentally the cause of the low efficiency of the Savonius rotor focusing on the vortex that is generating during rotation using a blade with slit. On the other hand, the research on the numerical simulation about S-shaped rotor is a few.⁽⁶⁾

In this paper, the numerical simulation is conducted about the simple structure S-shaped rotor with the slit near the tip of the blade to understand the flow around the rotor and the characteristics of the rotor by the torque.

2. Preparation of the calculation

2.1 Blade shape of the S-shaped rotor

The blade cross-section is axially symmetric with respect to the rotation axis, and the shape is semi-circular. The angle α is defined by the centre position of the slit shown in Fig 2. Table 1 shows the conditions of α . The slit width d is about 2.2% of the blade length L ($L = 2\pi R / 2$) under the condition of the Slit No.01-06, and about 2.8% under the condition of the Slit No.08-10.

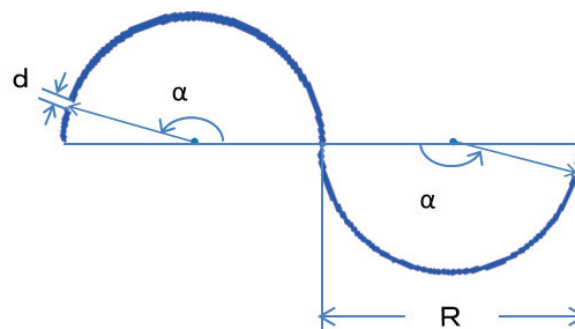


Fig. 2 Slit position

R: Rotor radius

d: Slit width

α : Slit angle

Table 1 Slit position

Slit No.	00	01	02	03	04	05	06	08	10
α [deg]	Without slit	170	166	162	158	154	148	139	129

2.2 computational grid

Figure 3 shows the computational grid. In this figure, the line are drawn every three to be shown clearly. The number of the grid point is 189×153 , and the computational domain is about 15 times in the X-axial direction and about 12 times in the Y-axis direction, relative to the diameter 1 of the rotor. The grid is generated by dividing the all regions into the several parts as shown in Fig.4, and each part are generated by using the transfinite interpolation method. The same grid is also used in the calculation for the blade with slit, and the slit is treated as the vacant part of the blade.

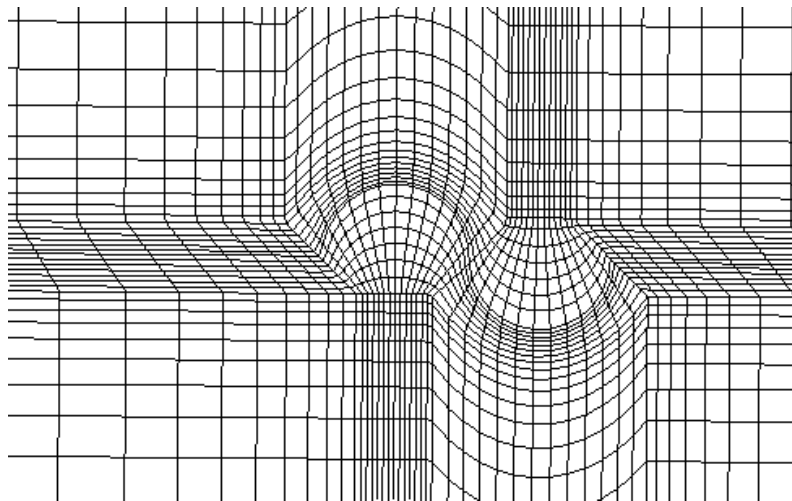


Fig. 3 Grid generation

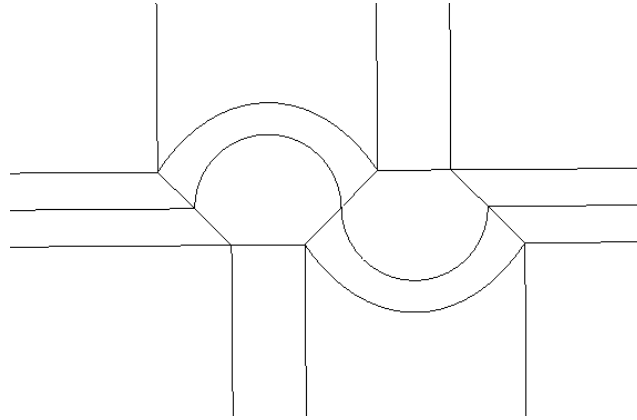


Fig. 4 Regions for the transfinite interpolation

2.3 Governing equation

Since the rotation speed is not high, the flow is governed by the incompressible Navier-Stokes equations. In this study, the calculation region is assumed to be two-dimensional and the calculation is conducted in a cross section perpendicular to the axis. The rotor is assumed to rotate at a constant angular velocity ω , and the coordinate system is the rotating coordinate system fixed to the blade. The relationship between the rotating coordinate system X - Y , U - V and the stationary coordinate system x - y , u - v are as follows where $\theta = \omega t$ is rotation angle.

$$\begin{aligned} X &= x \cos \theta - y \sin \theta \\ Y &= x \sin \theta + y \cos \theta \\ U &= u \cos \theta - v \sin \theta - \omega Y \\ V &= u \sin \theta + v \cos \theta + \omega X \end{aligned}$$

The continuity equation and the equation of motion that are expressed in the rotating coordinate system are as follows.

The continuous equation

$$\frac{\partial U}{\partial X} + \frac{\partial V}{\partial Y} = 0$$

The equation of motion

$$\frac{\partial U}{\partial t} + U \frac{\partial U}{\partial X} + V \frac{\partial U}{\partial Y} - \omega^2 X + 2\omega V = -\frac{\partial p}{\partial X} + \frac{1}{\text{Re}} \left(\frac{\partial^2 U}{\partial X^2} + \frac{\partial^2 U}{\partial Y^2} \right)$$

$$\frac{\partial V}{\partial t} + U \frac{\partial V}{\partial X} + V \frac{\partial V}{\partial Y} - \omega^2 Y - 2\omega U = -\frac{\partial p}{\partial Y} + \frac{1}{\text{Re}} \left(\frac{\partial^2 V}{\partial X^2} + \frac{\partial^2 V}{\partial Y^2} \right)$$

U, V : relative velocity

p: dynamic pressure

Re: Reynolds number

The fractional step method is used to solve them. The central difference are used to approximate the finite difference except the nonlinear terms, the nonlinear term is approximated by the upstream difference of the third-order accuracy. The wind speed u_{∞} is defined at infinity and the pressure is extrapolated, at the boundary of the blade. The Reynolds number Re is fixed to 2000 based on the rotor radius R and the wind speed u_{∞} .

3. Results and Discussions

3.1 The torque coefficient

The torque coefficient is calculated from the pressure applied to the blade. As an example, the time variation of the torque coefficient in the one cycle at the tip speed ratio of 1.0 without the slit which is the condition of the Slit No.00 is shown in Fig.5 and with the slit of the slit No.03 is shown in Fig.6. The variation of the torque coefficient is periodic, and in every conditions it takes the maximum value in the vicinity of $\theta = 30 + 180 \times n$ [deg] ; $n = 0, 1, 2, \dots$ and the minimum value in the vicinity of $\theta = 120 + 180 \times n$ [deg]. When the torque coefficient is a positive value, the rotation force is applying to the blade.

Figure 7 shows the relation between the tip speed ratio and the torque coefficient at the each slit conditions. The calculation are conducted using the torque coefficient value after the rotation is stabilized at the lap 16 (5760[deg]) to the lap 31(11520 [deg]).

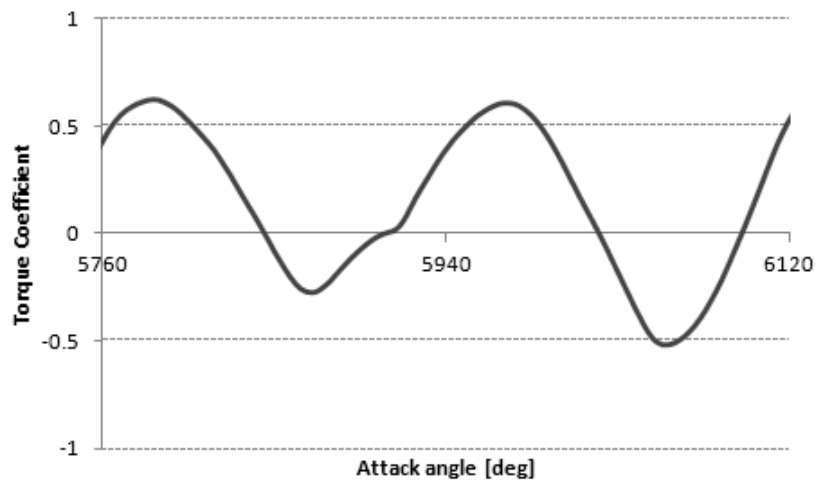


Fig. 5 The variation of the torque coefficient (Slit No.00, $\lambda = 1.0$)

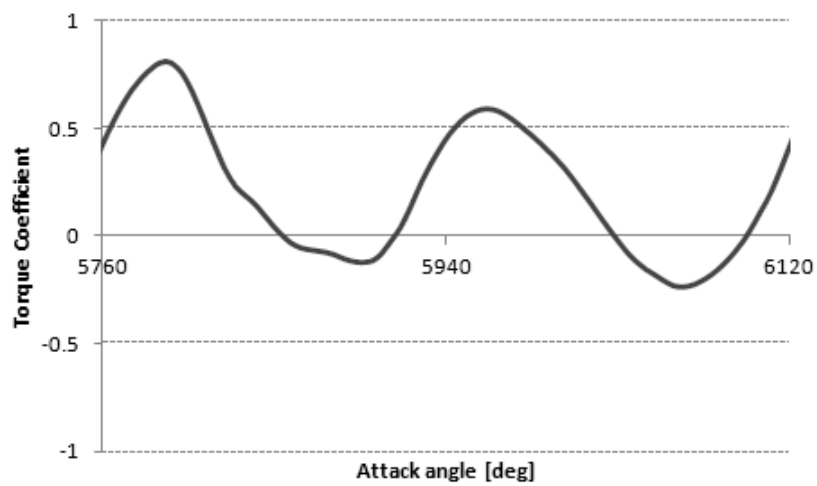


Fig. 6 The variation of the torque coefficient (Slit No.03, $\lambda = 1.0$)

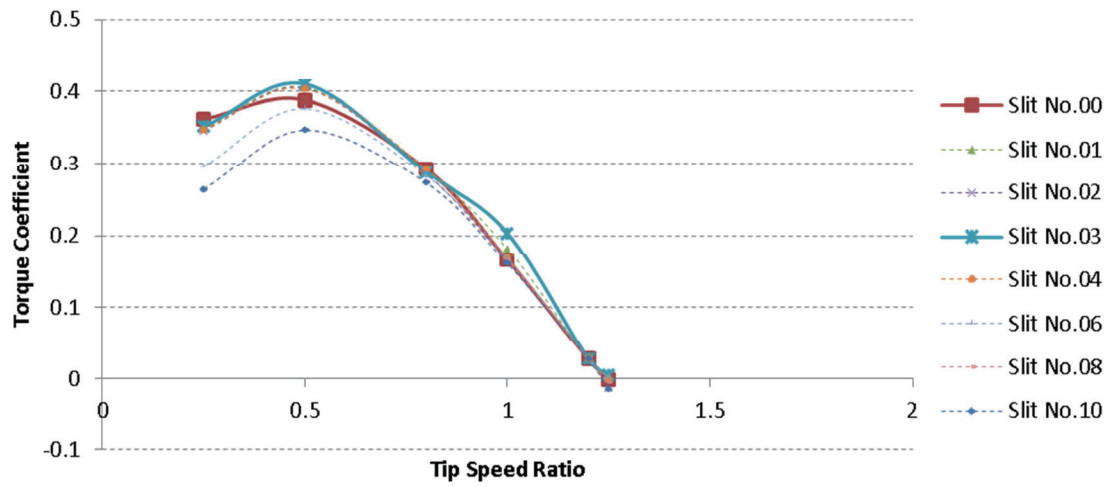


Fig. 7 Effect of slits on torque coefficients

3.2 The power coefficient

Figure 8 shows the relationship between the tip speed ratio and the power coefficient in each slit conditions. Ishimatsu et al⁽³⁾ calculated the two-dimensional S-shaped rotor using a different technique. Our result is almost identical qualitatively with their result at the tip speed ratio less than 1.0.

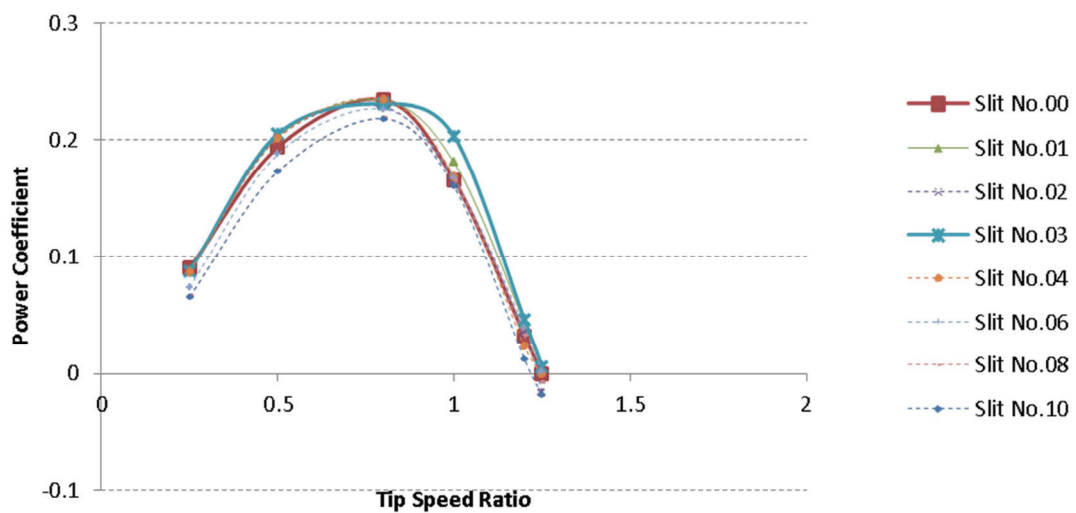


Fig. 8 Effect of slits on power coefficients

As the result of this study that is compared the calculation results of the blade with the slit and the no-slit, the following can be pointed out.

- It takes the maximum value of the power coefficient at the tip speed ratio of 0.8 in all the conditions.
- The conditions of the Slit No.01, 02, 03 and 04 have the slightly large power coefficient at the tip speed ratio of 0.5.
- At the tip speed ratio of 0.8, the conditions of the Slit No.01 and 04 have the almost same power coefficient, and the power coefficient are decreased in the other conditions.
- At the tip speed ratio of 1.0, the value of the power coefficient is increased approximately 25.0% in the condition of the Slit No.03 and also increased about 12.5% in the condition of the Slit No.01.

Yokomizo et al⁽⁵⁾ has been obtained the maximum power coefficient value at the $\alpha=165$ [deg] in their experimental investigation of the Savonius rotor with the slit. Our study has been also obtained the maximum value at $\alpha=162$ [deg], therefore the results of the both study are consistent that the power coefficient can be improved by providing the slit in this region.

3.3 The flow field

The power coefficient is improved at the tip speed ratio of 1.0, by comparing the results of the slit No.03 with the slit to that of the Slit No.00 without slit. Figure 9 shows the pressure contour and Fig. 10 shows the velocity vectors. Although the flow fields are nearly the same, the size of vortex that was generated on the advancing blade is smaller than that of the vortex on the blade with the slit.

Figure.11 and 12 show the distribution of the torque which is acquired on one side of the blade. Figure 11 indicates that the blade can get the maximum torque at $\theta=5780$ [deg]($20+180*n$ [deg], $n=0, 1, 2, \dots$). The torque of the blade in the condition of the Slit No.03 is higher than that of the Slit No.00 around the grid number of 20 i.e. near the center of the blade. Fig.12 indicates that the blade can get the minimum torque at $\theta=5870$ [deg] ($110+180*n$ [deg]). The torque in the condition of the Slit No.03 is also higher than that of the Slit No.00. In the presence of the slit, the torque in the direction that prevents the rotation force applied to the backside of the advancing blade is decreased and the high power coefficient is obtained.

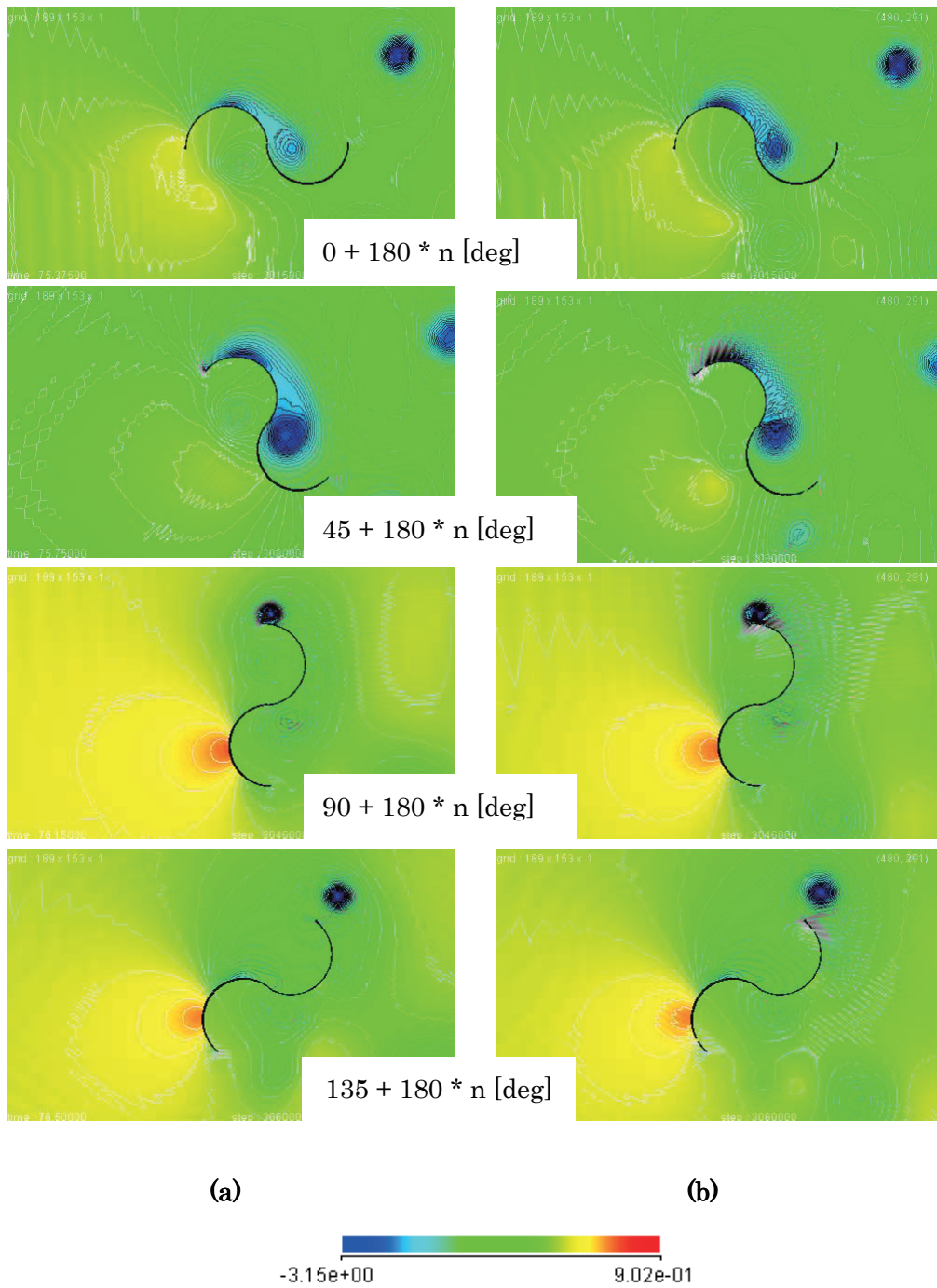


Fig.9 The pressure contour of the flow field
(a)Slit No.00, $\lambda = 1.0$, (b) Slit No.03, $\lambda = 1.0$. $n=0, 1, 2, \dots$

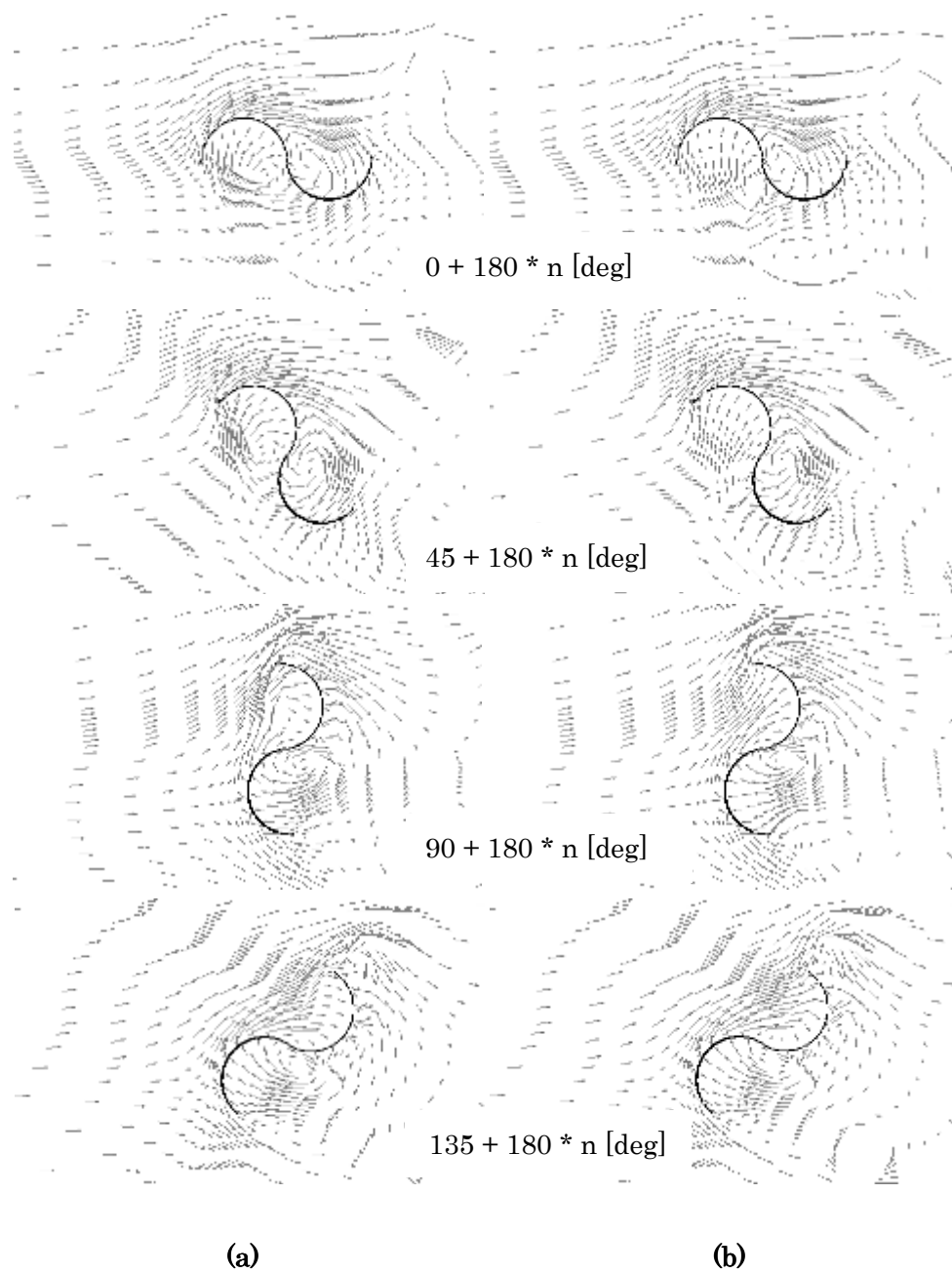


Fig.10 The vector of the flow field
(a)Slit No.00, $\lambda=1.0$, (b) Slit No.03, $\lambda=1.0$. $n=0, 1, 2, \dots$

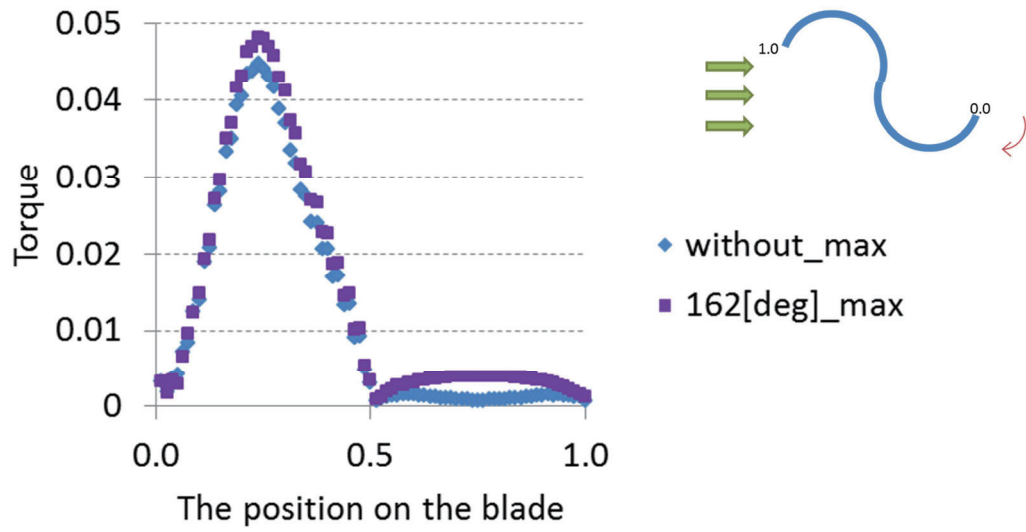


Fig. 11 Torque distribution ($\theta = 5780; 20 + 180 \cdot n$ [deg], $n=0, 1, 2, \dots$)

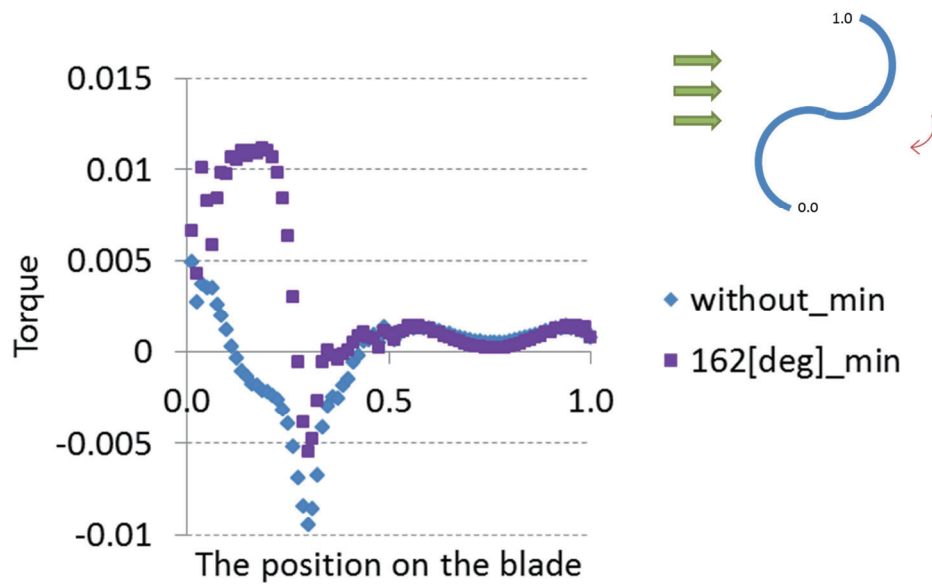


Fig. 12 Torque distribution ($\theta = 5870; 110 + 180 \cdot n$ [deg], $n=0, 1, 2, \dots$)

4. Conclusions

In this study, the flow field and the torque are examined about the S-shaped rotor with the slit provided to the blade by the numerical simulations. As the results, the following are found.

- (1) The improvement of overall power coefficient is possible by providing the slit in the vicinity of $\alpha = 162$ [deg].
- (2) The reason of the power coefficient improvement is the suppression of the vortex generation that inhibits the rotation, by providing the slit.

References

- [1] S.J.Savonius, The S-rotor and its application, *Mechanical Engineering*, 53(5), 333-338, 1931
SAVONIUS WIND TURBINES, Proceedings of the Seventeenth Intersociety Energy Conversion Engineering Conference, 4, 2096-2101, 1982
- [3] K.Ishimatsu, T.Shinohara and F.Takuma, Numerical simulation for Savonius rotors (running performance and flow fields), *JSME(B)*, 60(569), 154- 160, 1994
- [4] Ishimatsu Katsuya, Shinohara Toshio, Kage Kazuyuki and Okubayashi Toyoyasu, Numerical Simulation for Savonius Rotors : Effects of Shed Vortices on Running Performance, *JSME(B)*, 61(581), 12-17, 1995
- [5] Yokomizo Toshio and Ohta Genichi, Performance of Savonius Rotor with Slits in the Blades, *JSME(B)*, 59(568), 3854-3860, 1993
- [6] Anna Kuwana, Yuko Sato, Tetuya Kawamura, Numerical simulation for modified S-shaped wind turbines, Kyoto University Research Information Repository, 1539, 43-50, 2006

Yuka yoshida

Otsuka 2-1-1, Bunkyo-ku, Tokyo 112-8610, Japan

Shin-Nakahara-Cho 1, Isogo-ku, Yokohama 235-8501, Japan

e-mail: yuka_yoshida@ihi.co.jp

Tetuya Kawamura

Otsuka 2-1-1, Bunkyo-ku, Tokyo 112-8610, Japan

e-mail: kawamura@is.ocha.ac.jp